Robust Disturbance Rejection Control for Attitude Tracking of an Aircraft

Lu Wang and Jianbo Su

***Abstract*— This brief proposes a disturbance rejection control strategy for attitude tracking of an aircraft with both internal uncertainties and external disturbances. The proposed control strategy consists of a robust disturbance observer (DOB) and a nonlinear feedback controller. Specifically, a robust DOB is proposed to compensate the uncertain rotational dynamics into a nominal plant, based on which a nonlinear feedback controller is implemented for desired tracking performance. We first divide the practical rotational dynamics into the nominal part, external disturbances, and equivalent internal disturbances. Then, property of equivalent internal disturbances is explored for stability analysis. A robust DOB is optimized based on H_∞ theory to guarantee disturbance rejection performance and robustness against system uncertainties. A practical nonlinear feedback controller is hence applied to stabilize the compensated system based on backstepping approach. Experiments on a quadrotor testbed show that the proposed robust DOB can suppress the external disturbances and measurement noise, with the robustness against system uncertainties.**

***Index Terms*— Aircraft, attitude tracking, disturbance observer (DOB), disturbance rejection control, robust stability.**

I. Introduction

RESEARCH on aircraft control has been widely concerned with its applications, such as aerial inspection, satellite surveillance, geological survey, and rescue in disasters. For an aircraft, attitude control performance is essential in almost all these missions. Hence, development of a high-performance attitude control is an important and challenging work. Several approaches have been developed for the attitude stabilization or tracking problem [1]–[5]. Generally speaking, these control schemes are proposed with accurate system model. The system uncertainties are not considered.

Attitude tracking performance is usually affected by system uncertainties, such as unknown parameters of mass and inertia, actuators' uncertainties, and compound aerodynamic disturbances. To resolve these problems, numerous approaches have been proposed, such as sliding mode control [6], [7], adaptive control [8], robust control [9], linear quadratic regulation [10], nonlinear disturbance observer (DOB) [11], neural network [12], and fuzzy system [13]. These schemes can deal with the system uncertainties, as expected. However, it is still inevitable to face chattering of sliding mode control, convergence rate of weights in neural network and fuzzy system, and high gain of nonlinear DOB. Meanwhile, analysis of the methods mentioned above are carried out in time domain, which may be affected by the measurement noise with high frequency from the sensors.

Based on the above descriptions, we employ a DOB to compensate for the system uncertainties in attitude tracking control. DOB-based control method was originally proposed by Ohnishi [14] for linear single-input-single-output system, whose effectiveness in disturbance rejections has been shown in many applications [15]–[18]. DOB consists of a nominal model and a low-pass filter named Q filter, which is critical for system performance. Traditional DOB configuration in aircraft is affected by its nonlinearity and coupling property. A nonlinear control structure with DOB was proposed for nonlinear servo system, whose input to state stability was proven in [19]. However, a simple low-pass filter was adopted as the Q filter, whose performance was largely limited by its relative order and parameters. Meanwhile, as an important issue of DOB, robust stability condition against system uncertainties was not considered. A mixed sensitivity function with Q filter was established in [20] and [21] based on disturbance rejection and stability requirements, thus, standard H_∞ method was introduced to optimize the Q filter. However, this method can only be applied in linear systems.

In this brief, the control scheme based on linear DOB and nonlinear controller for a rotational rigid body system with strong coupling properties is investigated. A disturbance rejection control scheme is implemented to deal with the system uncertainties. The system error model is first established based on modified Rodrigues parameters (MRPs) and the uncertainties of actuators are considered. The rotational dynamics is divided into nominal part, external disturbances, and equivalent internal disturbances. Hence, property of internal uncertainties is explored, based on which the robust stability constraint is given. Then, we consider the robust stability, relative order, and mixed sensitivity requirements together to establish an optimization function, based on which the state-space solution in H_∞ control [22] is introduced to optimize the Q filter. Consequently, the uncertain dynamics can be compensated into a nominal plant, by which a backstepping approach is applied for desired tracking performance. Experiments are carried out on a quadrotor aircraft to verify the robustness against internal uncertainties as well as suppression of external disturbances of the directly designed DOB.

The rest of this brief is organized as follows. In Section II, the attitude control problem is presented to establish the system error model based on MRPs, and the property of internal uncertainties is analyzed. In Section III, a robust DOB is designed systematically based on H_∞ theory, and a nonlinear

Manuscript received May 29, 2014; revised October 11, 2014; accepted December 27, 2014. Manuscript received in final form January 25, 2015. This work was supported by the National Natural Science Foundation of China under Grant 61221003. Recommended by Associate Editor L. Marconi.

The authors are with the Key Laboratory of System Control and Information Processing, Department of Automation, Ministry of Education, Shanghai Jiao Tong University, Shanghai 200240, China (e-mail: wanglu1987xy@sjtu.edu.cn; jbsu@sjtu.edu.cn).

Digital Object Identifier 10.1109/TCST.2015.2398811

feedback control law is addressed to acquire desired tracking performance. Then, we analyze Lyapunov stability of the closed-loop system. In Section IV, a quadrotor aircraft testbed is introduced to verify the effectiveness of the proposed control scheme, followed by the conclusion in Section V.

II. System Model and Problem Formulation

A. System Model

There are three coordinate systems used in this brief, geographic coordinates $\mathcal{F}_e$, body-fixed coordinates $\mathcal{F}_b$, and orientated coordinates $\mathcal{F}_d$. We choose MRPs to represent the attitude. MRPs is a 3-D vector without restrictions, which is defined as $\boldsymbol{\sigma} = \boldsymbol{r}\tan(\alpha/4)$, where $\boldsymbol{r}$ and α represent the unit vector of rotational axis and rotation angle of the body frame, respectively. According to the definition of MRPs, its kinematics is given as

$$\dot{\boldsymbol{\sigma}} = G(\boldsymbol{\sigma})\boldsymbol{\omega} \tag{1}$$

where $\boldsymbol{\omega} \in \mathbb{R}^3$ denotes the angular velocity of the rigid body and the matrix $G(\boldsymbol{\sigma})$ is given as

$$G(\boldsymbol{\sigma}) = \frac{1}{2}\left(\frac{1-\boldsymbol{\sigma}^T\boldsymbol{\sigma}}{2}I_3 + [\boldsymbol{\sigma}\times] + \boldsymbol{\sigma}\boldsymbol{\sigma}^T\right) \tag{2}$$

where I_3 denotes the identity matrix with a dimension of three by three, $[\boldsymbol{\sigma}\times]$ denotes the skew-symmetric matrix of $\boldsymbol{\sigma}$. Concerning with the MRPs problem, please see [23] for further details.

The aircraft is considered as a rigid body without deformation, and the system model is described as

$$\begin{cases} \dot{\boldsymbol{\sigma}} = G(\boldsymbol{\sigma})\boldsymbol{\omega} \\ J\dot{\boldsymbol{\omega}} = -\boldsymbol{\omega}\times J\boldsymbol{\omega} + F\boldsymbol{u} \end{cases} \tag{3}$$

where $\boldsymbol{u} = [u_1\ u_2\ u_3]^T \in \mathbb{R}^3$ is the control input of the rotational dynamics, which can be regarded as the control surface or propeller speed of an aircraft. F is a 3-D input matrix, where $F\boldsymbol{u}$ is the control torque, and $J \in \mathbb{R}^{3\times3}$ is a symmetric square positive definite inertia matrix.

Assumption 1: Since matrix F is determined by structure and actuators of the aircraft, we assume that the aircraft is fully actuated, whose number of actuators is the same as its degrees-of-freedom. That is, the system model in (3) has an invertible F.

B. Problem Formulation

We consider the attitude tracking problem of an aircraft with the desired attitude $[\boldsymbol{\sigma}_d\ \boldsymbol{\omega}_d\ \dot{\boldsymbol{\omega}}_d]$ in orientated frame $\mathcal{F}_d$, denoting MRPs, angular velocity, and angular acceleration, respectively. The desired angular velocity $\boldsymbol{\omega}_d$ and desired angular acceleration $\dot{\boldsymbol{\omega}}_d$ are all bounded signals.

The orthogonal attitude transition matrix is denoted by $R \in SO(3)$, which is described as

$$R = I_3 - \frac{4(1-\boldsymbol{\sigma}^T\boldsymbol{\sigma})}{(1+\boldsymbol{\sigma}^T\boldsymbol{\sigma})^2}[\boldsymbol{\sigma}\times] + \frac{8}{(1+\boldsymbol{\sigma}^T\boldsymbol{\sigma})^2}[\boldsymbol{\sigma}\times]^2. \tag{4}$$

The relative MRPs and angular velocity variables from body-fixed frame $\mathcal{F}_b$ to the orientated frame $\mathcal{F}_d$ are defined as

$$\tilde{\boldsymbol{\sigma}} = \boldsymbol{\sigma} \oplus \boldsymbol{\sigma}_d^{-1}, \quad \tilde{\boldsymbol{\omega}} = \boldsymbol{\omega} - \tilde{R}\boldsymbol{\omega}_d \tag{5}$$

where $\boldsymbol{\sigma}_d^{-1}$ is the inverse of $\boldsymbol{\sigma}_d$, which is extracted as $\boldsymbol{\sigma}_d^{-1} = -\boldsymbol{\sigma}_d$, and $\tilde{R} = RR_d^T$ is known as the error of attitude transition matrix. The operator $\oplus$ denotes the production of MRPs as shown in (6) with two MRPs vectors of $\boldsymbol{\sigma}_1$ and $\boldsymbol{\sigma}_2$

$$\boldsymbol{\sigma}_1 \oplus \boldsymbol{\sigma}_2 = \frac{(1-\|\boldsymbol{\sigma}_2\|^2)\boldsymbol{\sigma}_1 + (1-\|\boldsymbol{\sigma}_1\|^2)\boldsymbol{\sigma}_2 - 2\boldsymbol{\sigma}_1\times\boldsymbol{\sigma}_2}{1+\|\boldsymbol{\sigma}_2\|^2\|\boldsymbol{\sigma}_1\|^2 - 2\boldsymbol{\sigma}_2^T\boldsymbol{\sigma}_1}. \tag{6}$$

Lemma 1 [24]: If attitude variable pairs $(\boldsymbol{\sigma}, \boldsymbol{\omega})$ and $(\boldsymbol{\sigma}_d, \boldsymbol{\omega}_d)$ both satisfy the MRPs kinematics, then the relative attitude variable pair also satisfies the MRPs kinematics.

From Lemma 1 and the definition of $\tilde{\boldsymbol{\omega}}$, we obtain the following rotational error model:

$$\begin{cases} \dot{\tilde{\boldsymbol{\sigma}}} = G(\tilde{\boldsymbol{\sigma}})\tilde{\boldsymbol{\omega}} \\ \dot{\tilde{\boldsymbol{\omega}}} = J^{-1}[-(\tilde{\boldsymbol{\omega}} + \tilde{R}\boldsymbol{\omega}_d)\times J(\tilde{\boldsymbol{\omega}} + \tilde{R}\boldsymbol{\omega}_d) + F\boldsymbol{u}] \\ \qquad -(\tilde{R}\dot{\boldsymbol{\omega}}_d - [\tilde{\boldsymbol{\omega}}\times]\tilde{R}\boldsymbol{\omega}_d). \end{cases} \tag{7}$$

Define the nominal inertia is J_0 and inertia error as $\Delta J = J - J_0$. Meanwhile, the nominal value of F is given as F_0, and its error is defined as $\Delta F = F - F_0$. Then, we can use the feedback linearization

$$\boldsymbol{u} = \boldsymbol{v} + F_0^{-1}L(\tilde{\boldsymbol{\omega}} + \tilde{R}\boldsymbol{\omega}_d)\mathrm{vec}(J_0) + F_0^{-1}J_0(\tilde{R}\dot{\boldsymbol{\omega}}_d - [\tilde{\boldsymbol{\omega}}\times]\tilde{R}\boldsymbol{\omega}_d) \tag{8}$$

to reduce the system dynamics to

$$F_0^{-1}J_0\dot{\tilde{\boldsymbol{\omega}}} = \boldsymbol{v} + \boldsymbol{d} + \boldsymbol{f} \tag{9}$$

where the definition of the operator $L(\cdot)$ and $\mathrm{vec}(\cdot)$ satisfy $L(\tilde{\boldsymbol{\omega}} + \tilde{R}\boldsymbol{\omega}_d)\mathrm{vec}(J_0) = (\tilde{\boldsymbol{\omega}} + \tilde{R}\boldsymbol{\omega}_d)\times J_0(\tilde{\boldsymbol{\omega}} + \tilde{R}\boldsymbol{\omega}_d)$, operator $\mathrm{vec}(\cdot)$ is a vector that contains all the components of the symmetric square matrix.

The external disturbances $\boldsymbol{d}$ satisfy Assumption 2, $\boldsymbol{f}$ is the internal uncertainties, and for $\delta \triangleq (FF_0)^{-1}(F_0\Delta J - \Delta F J_0)$, we have

$$\boldsymbol{f} = -[\delta\dot{\tilde{\boldsymbol{\omega}}} + L(\tilde{\boldsymbol{\omega}} + \tilde{R}\boldsymbol{\omega}_d)\mathrm{vec}(\delta) + \delta(\tilde{R}\dot{\boldsymbol{\omega}}_d - [\tilde{\boldsymbol{\omega}}\times]\tilde{R}\boldsymbol{\omega}_d)]. \tag{10}$$

Assumption 2: The external disturbances $\boldsymbol{d}$ are bounded signals with $\|\boldsymbol{d}\| < \bar{d}$.

All the analysis in the rest is presented based on the above rotational error model. From (4), we obtain $\tilde{R} = I_3$ when $\tilde{\boldsymbol{\sigma}} = 0$. From the orthogonality of attitude matrix, $\tilde{R} = I_3$ if and only if $R = R_d$. Then, due to the definition of $\tilde{\boldsymbol{\omega}}$, we obtain $\boldsymbol{\omega} = \boldsymbol{\omega}_d$ while $\tilde{R} = I_3$ and $\tilde{\boldsymbol{\omega}} = 0$. This implies that stabilizing the error system in (7) is equivalent to the objective of attitude tracking. Hence, the control objective turns to design a controller for stabilization of equilibrium point: $\tilde{\boldsymbol{\sigma}} = 0, \tilde{\boldsymbol{\omega}} = 0$, with existence of external disturbances and system uncertainties.

C. Analysis of System Uncertainties

Consider the expression of the internal uncertainties $\boldsymbol{f}$ in (10) and introduce the notation

$$\boldsymbol{f}_1 = -L(\tilde{\boldsymbol{\omega}} + \tilde{R}\boldsymbol{\omega}_d)\mathrm{vec}(\delta) - \delta(\tilde{R}\dot{\boldsymbol{\omega}}_d - [\tilde{\boldsymbol{\omega}}\times]\tilde{R}\boldsymbol{\omega}_d). \tag{11}$$

Since $\|\tilde{R}\|$, $\|\boldsymbol{\omega}_d\|$, and $\|\dot{\boldsymbol{\omega}}_d\|$ are all bounded, from the definition of $\|\boldsymbol{f}_1\|$, there exists a standard $\mathcal{K}$ function $\alpha(\cdot)$

and a positive constant η such that $\|\boldsymbol{f}_1\| < \alpha(\|\tilde{\boldsymbol{\omega}}\|) + \eta$. From the definition of $L(\cdot)$, we know that the first part of $\boldsymbol{f}_1$ is of the second order for input $\tilde{\boldsymbol{\omega}}$, which means $\mathcal{K}$ function $\alpha(\cdot)$ is of the second order.

By substituting (9) into (10), it follows that

$$\boldsymbol{f} = \left(I_3 + \delta J_0^{-1} F_0\right)^{-1}\left[-\delta J_0^{-1} F_0(\boldsymbol{v} + \boldsymbol{d}) + \boldsymbol{f}_1\right]. \tag{12}$$

Since external disturbances $\boldsymbol{d}$ are bounded and by considering the property of $\boldsymbol{f}_1$ and feedback controller $\boldsymbol{v}$, there exist $\mathcal{K}$ functions $\alpha_1(\cdot), \alpha_2(\cdot), \alpha_3(\cdot)$ and a positive constant $\bar{\eta}$ such that

$$\|\boldsymbol{f}\| \leq \alpha_1(\|\tilde{\boldsymbol{\sigma}}\|) + \alpha_2(\|\tilde{\boldsymbol{\omega}}\|) + \alpha_3(\|\hat{\boldsymbol{d}}\|) + \bar{\eta}. \tag{13}$$

The previous property of system uncertainties can be applied to obtain the Lyapunov stability. Consider the existing works in the robust stability analysis of DOB-based control structure in [15], [17], and [20], we can design the sensitivity function of Q filter based on small gain theorem for robust stability. Hence, the system dynamics is transformed into the form with multiplicative uncertainty. The multiplicative uncertainty $\Delta(s)$ is given as

$$\Delta(s) = P_n^{-1}(s)(P(s) - P_n(s)) \tag{14}$$

where $P(s)$ and $P_n(s)$ are the real and nominal models of the rotational dynamics, respectively. By substituting the upper bound of $\boldsymbol{f}(s)$ into (14), we can obtain the upper bound of $\Delta(s)$ for robust stability.

Converting the description of $\boldsymbol{f}$ into frequency domain using Laplace transform, we can obtain its upper bound from (10)

$$f(s) = (-\delta s + \alpha_0)\tilde{\boldsymbol{\omega}} + \eta \tag{15}$$

for the selected $\alpha_0 = \sup_{\|\tilde{\boldsymbol{\omega}}\| < \omega_0}(\alpha(\|\tilde{\boldsymbol{\omega}}\|)/\|\tilde{\boldsymbol{\omega}}\|)$. s is the Laplace operator.

Consider that the input $\boldsymbol{v}$ consists of the state feedback of $\tilde{\boldsymbol{\omega}}$, which will in turn change the poles of the rotational dynamics. Hence, the feedback controller should be considered to acquire the nominal model $P_n(s)$. Since the calculation of $P_n(s)$ will be affected by the designed control law, design procedures are shown in Section IV.

III. Controller Design Based on Robust DOB

A. Control Structure

The control system is divided into two parts, an inner loop for the rotational dynamics and an outer loop for the whole feedback system, respectively. In the inner loop, we apply a DOB to eliminate the influence caused by the unknown external disturbances and internal parameters perturbation. The designed DOB should guarantee the robustness against the internal uncertainties. Since the system uncertainties have already been compensated, a nonlinear feedback controller is presented to stabilize the nominal error model. The control structure is shown in Fig. 1, where $\hat{\boldsymbol{d}}$ is the estimated disturbance of DOB.

For the error system dynamics expressed in (7), a DOB is designed to compensate it into a nominal plant. We consider the robust stability, relative order, and mixed sensitivity design requirements together to establish an optimization function. Then, the optimization problem is transformed into an H_∞ control problem, and the state-space solution in H_∞ control [22] can be employed directly to achieve the optimal solution. Hence, the outer loop controller is designed based on the nominal error model. To implement the controller conveniently in the embedded system, the practical nonlinear feedback technique is applied to design the outer loop controller.

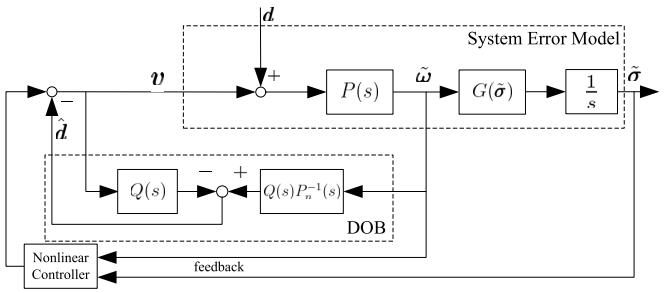

Fig. 1. Control structure of the closed-loop system.

B. Robust DOB Design

From the above review, we know that the key point of DOB is the design of Q filter and it must satisfy the following.

1) The relative order of $Q(s)$ should be higher than or at least equal to that of $P_n(s)$ to make sure $Q(s)P_n^{-1}(s)$ is proper.
2) Selection of Q filter should suppress the external disturbances. If there is no prior information of the external disturbances, we can regard them as the load disturbances.
3) The robust stability of the closed-loop system should be satisfied.

Consequently, the optimization function is established based on the above requirements. The transfer function of the inner loop is expressed as

$$\begin{aligned}\tilde{\boldsymbol{\omega}} = &[P_n(s) + P(s)Q(s) - P_n(s)Q(s)]^{-1} \\ &\times [P(s)P_n(s)\boldsymbol{u} + (1 - Q(s))P(s)P_n(s)\boldsymbol{d}].\end{aligned} \tag{16}$$

A set of $Q(s)$ is defined as

$$\Omega_k = \left\{F(s) | F(s) = \frac{\sum_{j=0}^{m} b_j s^j}{\sum_{i=0}^{n} a_i s^i}, \quad k = n - m\right\} \tag{17}$$

where k is the relative order mentioned above.

From (16), we notice that $1 - Q(s)$ should be as small as possible to attenuate disturbance $\boldsymbol{d}$, the optimization function that reflects the disturbance rejection performance is given as

$$\min_{Q(s)} \|W_1(s)(1 - Q(s))\|_\infty \tag{18}$$

where $W_1(s)$ is the weighting function that reflects the prior frequency property of the disturbances.

The designed Q filter should be robust against the system uncertainties. From [15], [17], and [20], the inner loop is robustly stable based on small gain theorem if

$$\|W_2(s)Q(s)\|_\infty \leqslant 1 \tag{19}$$

where $W_2^{-1}(j\varpi) < \Delta^{-1}(j\varpi), \forall\varpi$. Here, we use ϖ to denote the frequency signal.

From the above analysis, the disturbances rejection and robust stability problems can be regarded as a tradeoff between the sensitivity and complementary sensitivity functions. Hence, the optimization problem is given as

$$\begin{aligned}&\max \gamma\\ &\text{s.t.} \min_{\substack{Q(s)\in\Omega_k\\ Q(s)\in\mathcal{RH}_\infty}} \left\| \begin{bmatrix} \gamma\, W_1(s)(1-Q(s)) \\ W_2(s)Q(s) \end{bmatrix} \right\|_\infty < 1. \end{aligned} \tag{20}$$

The standard H_∞ method is proposed for this kind of optimization problem in [14]. By defining the transfer function of virtual loop as $\tilde{L}(s) = Q(s)/(1-Q(s)) = \tilde{P}(s)\tilde{K}(s)$, the Q filter design problem turns to be a standard H_∞ problem

$$\begin{aligned}&\max \gamma\\ &\text{s.t.} \min_{\substack{Q(s)\in\Omega_k\\ Q(s)\in\mathcal{RH}_\infty}} \left\| \begin{bmatrix} \gamma\, W_1(s)(I+\tilde{P}(s)\tilde{K}(s))^{-1} \\ W_2(s)\tilde{P}(s)\tilde{K}(s)(I+\tilde{P}(s)\tilde{K}(s))^{-1} \end{bmatrix} \right\|_\infty < 1 \end{aligned} \tag{21}$$

where $\tilde{L}(s) = \tilde{P}(s)\tilde{K}(s)$ and $\tilde{P}(s), \tilde{K}(s)$ are the virtual controlled objective and controller, respectively.

The standard state-space solution in H_∞ control can be applied to obtain the optimal solution. For a given virtual controlled objective $\tilde{P}(s)$, if we can acquire the optimal solution of the virtual controller $\tilde{K}(s)$, then the optimal Q filter can be obtained as

$$Q(s) = \frac{\tilde{P}(s)\tilde{K}(s)}{1+\tilde{P}(s)\tilde{K}(s)}. \tag{22}$$

Remark 1: Since $\tilde{K}(s)$ is proper and can eliminate all the poles of $\tilde{P}(s)$, $\tilde{L}(s)$ has the same relative order as that of $\tilde{P}(s)$, thus, $Q(s) \in \Omega_k$ if $\tilde{P}(s) \in \Omega_k$.

Remark 2: From the theory of H_∞ optimal control problem, the closed-loop system of virtual H_∞ control problem is internally stable, then $Q(s) = (\tilde{P}(s)\tilde{K}(s)/1 + \tilde{P}(s)\tilde{K}(s)) \in \mathcal{RH}_\infty$, that is, all the poles of $Q(s)$ are in the open left half of the s-plane.

C. Backstepping-Based Nonlinear Control

With the estimated disturbance of the proposed DOB, a backstepping-based nonlinear controller is designed as the torque input for attitude tracking performance.

To employ the backstepping technique for controller design, we first introduce $\tilde{\boldsymbol{\Omega}}$

$$\tilde{\boldsymbol{\Omega}} = \tilde{\boldsymbol{\omega}} + k_1\tilde{\boldsymbol{\sigma}} \tag{23}$$

where k_1 is a strictly positive matrix.

Consider the following candidate Lyapunov function V_1 as:

$$V_1 = 2\ln(1+\tilde{\boldsymbol{\sigma}}^T\tilde{\boldsymbol{\sigma}}) + \frac{1}{2}\tilde{\boldsymbol{\Omega}}^T\left(F_0^{-1}J_0\right)\tilde{\boldsymbol{\Omega}}. \tag{24}$$

Notice that $\boldsymbol{\sigma}^T G(\boldsymbol{\sigma}) = (1+\boldsymbol{\sigma}^T\boldsymbol{\sigma})/(4)\boldsymbol{\sigma}^T$, derivative of V_1 is described as

$$\dot{V}_1 = -\tilde{\boldsymbol{\sigma}}^T k_1\tilde{\boldsymbol{\sigma}} + \tilde{\boldsymbol{\sigma}}^T\tilde{\boldsymbol{\Omega}} + \tilde{\boldsymbol{\Omega}}^T\left(\boldsymbol{v} + \boldsymbol{d} + \boldsymbol{f} + k_1 J_0^{-1}F_0 G(\tilde{\boldsymbol{\sigma}})\tilde{\boldsymbol{\omega}}\right) \tag{25}$$

consequently, the control input $\boldsymbol{v}$ is proposed as

$$\boldsymbol{v} = -(1+k_1k_2)\tilde{\boldsymbol{\sigma}} - \left(k_2 + F_0^{-1}J_0k_1G(\tilde{\boldsymbol{\sigma}})\right)\tilde{\boldsymbol{\omega}} - \hat{\boldsymbol{d}} \tag{26}$$

where k_2 is a strictly positive matrix and $\hat{\boldsymbol{d}}$ is the estimated disturbances of DOB.

Define the estimating error of the DOB system as $\tilde{\boldsymbol{d}} = \boldsymbol{d} + \boldsymbol{f} - \hat{\boldsymbol{d}}$, then substituting (26) into (25) yields

$$\dot{V}_1 \le -\lambda_{\min}(k_1)\|\tilde{\boldsymbol{\sigma}}\|^2 - \lambda_{\min}(k_2)\|\tilde{\boldsymbol{\Omega}}\|^2 + \|\tilde{\boldsymbol{\Omega}}\|\|\tilde{\boldsymbol{d}}\|. \tag{27}$$

Assume that the estimating error of DOB is the input of the above system. Then, the unforced system is exponentially stable at the equilibrium point. From (8), the control torque of the attitude tracking problem is finally described as

$$\begin{aligned}\boldsymbol{u} =& -(1+k_1k_2)\tilde{\boldsymbol{\sigma}} - (k_2 + F_0^{-1}J_0k_1G(\tilde{\boldsymbol{\sigma}}))\tilde{\boldsymbol{\omega}} - \hat{\boldsymbol{d}}\\ &+ F_0^{-1}L(\tilde{\boldsymbol{\omega}} + \tilde{R}\boldsymbol{\omega}_d)\mathrm{vec}(J_0) + F_0^{-1}J_0(\tilde{R}\dot{\boldsymbol{\omega}}_d - [\tilde{\boldsymbol{\omega}}\times]\tilde{R}\boldsymbol{\omega}_d).\end{aligned} \tag{28}$$

D. Stability of the Closed-loop System

Stability of the closed-loop system with both internal uncertainties and external disturbances is analyzed based on Lyapunov theorem.

Theorem 1: Given a rotational error system of an aircraft in (7) for a desired attitude trajectory defined as $[\boldsymbol{\sigma}_d\ \boldsymbol{\omega}_d\ \dot{\boldsymbol{\omega}}_d]$. With the external disturbances $\boldsymbol{d}$ and internal uncertainties $\boldsymbol{f}$ in (10), let the Q filer of DOB optimized by (20) and nonlinear feedback controller defined by (28). Then, the MRPs error $\tilde{\boldsymbol{\sigma}}$, the angular velocity error $\tilde{\boldsymbol{\omega}}$, and the estimation error $\tilde{\boldsymbol{d}}$ of DOB are locally uniformly ultimately bounded (UUB).

Proof: We first establish the state equation of estimation error of DOB. From the control structure in Fig. 1, the estimated disturbance is

$$\hat{\boldsymbol{d}} = -Q(s)\boldsymbol{v} + Q(s)P_n^{-1}(s)\tilde{\boldsymbol{\omega}}. \tag{29}$$

Notice that $P_n^{-1}(s)\tilde{\boldsymbol{\omega}} = F_0^{-1}J_0\dot{\tilde{\boldsymbol{\omega}}}$, we obtain

$$\hat{\boldsymbol{d}} = -Q(s)\boldsymbol{v} + Q(s)F_0^{-1}J_0\dot{\tilde{\boldsymbol{\omega}}} = Q(s)(\boldsymbol{d}+\boldsymbol{f}). \tag{30}$$

We regard $(\boldsymbol{d}+\boldsymbol{f})$ as input of the DOB-based system. Simultaneously, $\hat{\boldsymbol{d}}$ and $\tilde{\boldsymbol{d}}$ are regarded as the output of DOB-based system. The state space of the inner loop based on DOB is expressed as

$$\begin{cases}\dot{\boldsymbol{z}} = A\boldsymbol{z} + B(\boldsymbol{d}+\boldsymbol{f})\\ \hat{\boldsymbol{d}} = C\boldsymbol{z}, \tilde{\boldsymbol{d}} = -C\boldsymbol{z} + (\boldsymbol{d}+\boldsymbol{f})\end{cases} \tag{31}$$

where $\boldsymbol{z}$ is the state of the DOB structure.

Remark 3: The specific form of A, B, C, and $\boldsymbol{z}$ are determined by the optimized Q filter. Here, we only know that (A, B, C) is a minimal realization of the DOB-based system. (A, B) is controllable, and (A, C) is observable. Since $Q(s) \in \mathcal{RH}_\infty$, the matrix A is Hurwitz. That is, for any given positive definite symmetric matrix N, there exists a positive definite symmetric matrix M such that $MA + A^TM = -N$.

By introducing a new Lyapunov function $V_2 = kV_1 + \boldsymbol{z}^TM\boldsymbol{z}$, its derivative is given as

$$\begin{aligned}\dot{V}_2 \le& -k\lambda_{\min}(k_1)\|\tilde{\boldsymbol{\sigma}}\|^2 - k\lambda_{\min}(k_2)\|\tilde{\boldsymbol{\Omega}}\|^2 + k\|\tilde{\boldsymbol{\Omega}}\|\|\tilde{\boldsymbol{d}}\|\\ &-\lambda_{\min}(N)\|\boldsymbol{z}\|^2 + 2\|M\|\|B\|\|\boldsymbol{z}\|(\bar{d} + \|\boldsymbol{f}\|).\end{aligned} \tag{32}$$

From the definition of $\tilde{\boldsymbol{\omega}}$, we notice that $(\tilde{\boldsymbol{\sigma}}, \tilde{\boldsymbol{\Omega}})$ is a linear diffeomorphism of $(\tilde{\boldsymbol{\sigma}}, \tilde{\boldsymbol{\omega}})$. Consequently, from the property of system uncertainties in Section II, we can observe that for any

compact set, if the system states are in this compact set, then there exist positive constants a_1–a_5 that satisfy

$$\|\boldsymbol{f}\| \le a_1\|\tilde{\boldsymbol{\sigma}}\| + a_2\|\tilde{\boldsymbol{\Omega}}\| + a_3\|\tilde{\boldsymbol{\Omega}}\|^2 + a_4\|\boldsymbol{z}\| + a_5. \quad (33)$$

Substituting (33) into (32) yields

$$\dot{V}_3 \le -c_1\|\tilde{\boldsymbol{\sigma}}\|^2 - c_2\|\tilde{\boldsymbol{\Omega}}\|^2 - c_3\|\boldsymbol{z}\|^2 + \mu \quad (34)$$

where

$$\begin{aligned}
c_1 &= k\lambda_{\min}(k_1) - \frac{ka_1}{2\lambda_2} - \frac{a_1\|M\|\|B\|}{\lambda_3} \\
c_2 &= \Bigg[k\lambda_{\min}(k_2) - \frac{k(\lambda_{\max}(C)+a_4)}{2\lambda_1} - \frac{ka_1\lambda_2}{2} - ka_2 \\
&\quad - \frac{a_2\|M\|\|B\|}{\lambda_4} - \frac{(k\bar{d})^2}{4\mu_1} - \frac{(ka_5)^2}{4\mu_2} \\
&\quad - ka_3\|\tilde{\boldsymbol{\Omega}}\| - \frac{a_3\|M\|\|B\|}{\lambda_5}\|\tilde{\boldsymbol{\Omega}}\|^2\Bigg] \\
c_3 &= \Bigg[\lambda_{\min}(N) - \frac{k\lambda_1(\lambda_{\max}(C)+a_4)}{2} - \frac{(\bar{d}\|M\|\|B\|)^2}{\mu_3} \\
&\quad - \frac{(a_5\|M\|\|B\|)^2}{\mu_4} - 2a_4\|M\|\|B\| \\
&\quad - \|M\|\|B\|(a_1\lambda_3 + a_2\lambda_4 + a_3\lambda_5)\Bigg] \\
\mu &= \mu_1 + \mu_2 + \mu_3 + \mu_4
\end{aligned}$$

where λ_1–λ_5 and μ_1–μ_4 are the positive constants.

It is assumed that $\Omega_0 > (\mu/c_2)^{1/2}$ is the upper bound of $\|\tilde{\boldsymbol{\Omega}}\|$ such that $c_2 > 0$. For $\|\tilde{\boldsymbol{\Omega}}(t_0)\| < \Omega_0$, $\dot{V}$ is strictly negative provided the following inequalities hold: $\|\tilde{\boldsymbol{\sigma}}\| > (\mu/c_1)^{1/2}$, or $\|\tilde{\boldsymbol{\Omega}}\| > (\mu/c_2)^{1/2}$, or $\|\boldsymbol{z}\| > (\mu/c_3)^{1/2}$. Then, the above three states are locally UUB and can converge into a compact set. Notice that $(\tilde{\boldsymbol{\sigma}}, \tilde{\boldsymbol{\Omega}})$ is a linear diffeomorphism of $(\tilde{\boldsymbol{\sigma}}, \tilde{\boldsymbol{\omega}})$. Hence, $(\tilde{\boldsymbol{\sigma}}, \tilde{\boldsymbol{\omega}})$ can converge into a compact set. From (31), it is easy to observe that the MRPs error, the angular velocity error, and the estimation error of DOB are locally UUB. □

IV. Experimental Results

A. Quadrotor Testbed

A quadrotor aircraft is applied to show the effectiveness of the proposed control strategy. A quadrotor is a kind of aircraft with the appearance of a dish. It consists of four independent motor driving systems that are bound together on a rigid criss-cross structure. The four rotors are located at the tips of the rigid body, and the rotors alternate between rotating clockwise and counterclockwise as you move around the system. The rotational rates of the rotors are identical during hovering. Conversely, changing the speeds of two propellers that are opposite to each other produces pitch or roll motion. Yaw motion results from the difference in the counter torque between each pair of propellers, which is caused by changing the speeds of two pairs of propellers conversely.

Define the control input as $\boldsymbol{u} = [\omega_\phi \ \omega_\theta \ \omega_\psi]^T$, then, the rotational speeds of each propellers are

$$\begin{cases} \omega_1 = \omega_T + \omega_\theta + \omega_\psi, & \omega_2 = \omega_T + \omega_\phi - \omega_\psi \\ \omega_3 = \omega_T - \omega_\theta + \omega_\psi, & \omega_4 = \omega_T - \omega_\phi - \omega_\psi \end{cases} \quad (35)$$

where ω_T is the nominal rotor speed required to hover.

TABLE I
Parameters of the Quadrotor Aircraft

Parameter	Value	Error	Unit
C_T	0.012	± 0.003	
C_Q	0.93×10^{-3}	$\pm 0.2 \times 10^{-3}$	
ρ	1.184		$Kg \cdot m^{-3}$
A	0.0515	± 0.002	m^2
r	0.128	± 0.001	m
l	0.25	± 0.01	m
J_ϕ	0.014	± 0.002	$Kg \cdot m^2$
J_θ	0.014	± 0.002	$Kg \cdot m^2$
J_ψ	0.024	± 0.004	$Kg \cdot m^2$
ω_T	215	± 5	rad/s

From the principle of the quadrotor aircraft, the control torque is shown as

$$F\boldsymbol{u} = \begin{bmatrix} C_T\rho A r^2 l\left(\omega_1^2 - \omega_3^2\right) \\ C_T\rho A r^2 l\left(\omega_2^2 - \omega_4^2\right) \\ C_Q\rho A r^3\left(\omega_1^2 + \omega_3^2 - \omega_2^2 - \omega_4^2\right) \end{bmatrix} \quad (36)$$

where C_T and C_Q are the coefficients of thrust and torque from rotational speed, respectively. ρ is the density of air, r is the propeller's radius, A is the propeller's disc area, and l is the rotor displacement from the quadrotor center of mass. Assume that the value of $\boldsymbol{u}$ is smaller than that of ω_T, we finally obtain the matrix F as

$$F = \mathrm{diag}(4C_T\rho A r^2 l\omega_T, 4C_T\rho A r^2 l\omega_T, 8C_Q\rho A r^3\omega_T).$$

Here, diag$(\cdot)$ denotes the diagonal matrix and the related parameters are shown in Table I, in which J_ϕ, J_θ and J_ψ are the correspondingly rotational inertia of three axes.

The control gains are chosen as $k_1 = 1.5$ and $k_2 = 9.0$, and according to the controller in (28), we obtain the rotational dynamics as

$$\begin{cases} \boldsymbol{f} = -\left[\delta\dot{\tilde{\boldsymbol{\omega}}} - L(\tilde{\boldsymbol{\omega}} + \tilde{R}\boldsymbol{\omega}_d)\mathrm{vec}(\delta) - \delta(\tilde{R}\dot{\boldsymbol{\omega}}_d - [\tilde{\boldsymbol{\omega}}\times]\tilde{R}\boldsymbol{\omega}_d)\right] \\ \left[F_0^{-1}J_0 s + \left(k_2 + F_0^{-1}J_0 k_1 G(\tilde{\boldsymbol{\sigma}})\right)\right]\tilde{\boldsymbol{\omega}} = \boldsymbol{v}' + \boldsymbol{d} + \boldsymbol{f} \end{cases} \quad (37)$$

where $\boldsymbol{v}'$ is the input of the rotational dynamics. The second equation in (37) can be regarded as the nominal plant perturbed by external disturbances $\boldsymbol{d}$ and internal uncertainties $\boldsymbol{f}$. Notice that $G(\tilde{\boldsymbol{\sigma}})$ approximates to a matrix $I_3/4$ near the equilibrium point, the transfer function $P(s)$ from $\boldsymbol{v}'$ to $\tilde{\boldsymbol{\omega}}$ is

$$P(s) = \left[\left(F_0^{-1}J_0 + \delta\right)s + \left(k_2 + F_0^{-1}J_0 k_1\right)\right]^{-1}. \quad (38)$$

The nonlinear terms in $\boldsymbol{f}$ are regarded as disturbance to be compensated for.

Without any prior information of the external disturbances, the weighting function for the disturbance rejection can be selected as $W_1(s) = 1/s^2$.

Since the quadrotor is axial symmetric, the corresponding parameters of pitch and roll axes are same. Hence, we only need to determine the weighting functions $W_2(s)$ for pitch (roll) axis and yaw axis. Fig. 2 shows the frequency responses of $\Delta(s)$ for different values of δ. It is also required that the designed Q filter has at least -20-dB attenuation against the

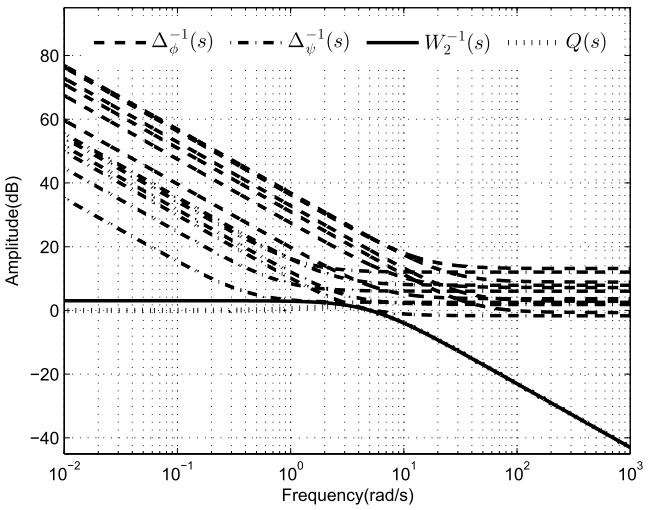

Fig. 2. System uncertainty and its restriction on Q filter.

Fig. 3. Quadrotor aircraft testbed.

measurement noise of gyroscope larger that 42 Hz. From the above description, the weighting function is defined as

$$W_2(s) = \frac{0.2s + 1}{1.42}. \tag{39}$$

Then, the virtual controller $\tilde{K}(s)$ is optimized through (21) by state-space solution in H_∞ control. The Q filter is obtained while $\gamma = 8.1$

$$Q(s) = \frac{7.1s + 11.415}{s^2 + 7.1s + 11.415}. \tag{40}$$

Our experimental platform is shown in Fig. 3. The mechanical structure of the aircraft is based on the material of carbon fiber. For the elaboration of the real-time flight control board, it consists of a microprocessor, an inertial measurement unit (IMU), and an electronic compass. The IMU, InvenSense's MPU6050, provides us with digital signal of three-axis angular velocities and accelerations. The electronic compass and Honeywell's HMC5883 gives the three-axis magnetic field of the rigid body. The microprocessor, STM32 ARM Cortex, is used to capture the signal data from the sensors and to implement the control strategy. A nonlinear complementary filter is implemented to estimate the attitude information and gyro bias [26]. The quadrotor aircraft testbed

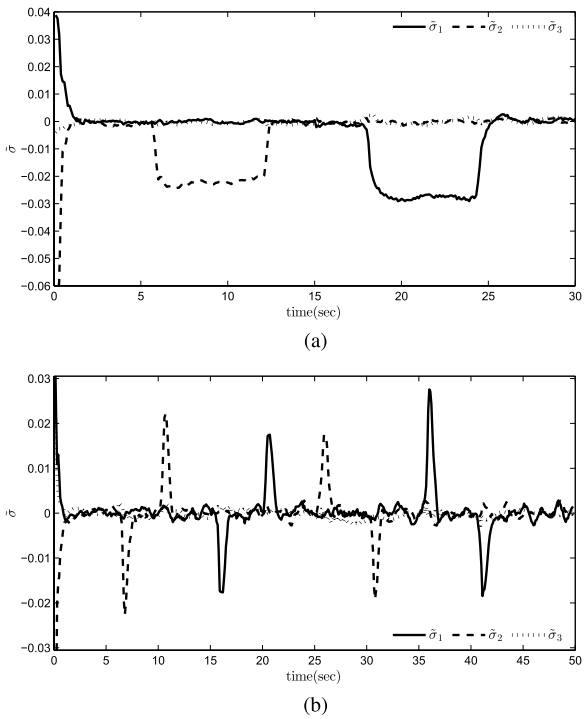

Fig. 4. Attitude stabilization performance. (a) Attitude stabilization without DOB. (b) Attitude stabilization with DOB.

is shown in Fig. 3. Four brushless dc motors are used to provide thrust and torque, with the power supported by a lithium polymer battery.

The sample rate of the experimental system is 200 Hz. Two experiments have been accomplished in this section. The attitude stabilization case is presented in the first experiment. Specifically, to test the disturbance rejection performance of the proposed scheme, a mass of 135 g is hung from each arm of the quadrotor structure, equivalent to a load disturbance of 0.0388 N · m in pitch or roll axis. In the second experiment, the attitude tracking problem is considered.

In this brief, the load disturbance is persistent for a few seconds in the experiments. Actually, the practical disturbance is usually persistent, for example, the persistent aerodynamic disturbance, mismatched center of gravity, and mismatched load. Hence, the load disturbance is introduced to validate the disturbance rejection ability, and robustness of the designed controller and DOB.

B. Attitude Stabilization

The attitude stabilization effects with and without DOB are compared in Fig. 4. The experimental results show that the controller can stabilize the attitude errors within 1 s. At about 6 and 17 s, the load disturbance mentioned above is hung on the pitch and roll axes, respectively. The designed controller cannot totally eliminate this disturbance without DOB. The MRP error remains until the external disturbance is removed.

Then, with the proposed DOB, we perturbed the load disturbance on quadrotor for a few seconds, and then removed it. This procedure is repeated for four times on each tip of the quadrotor. We notice that with the action of DOB,

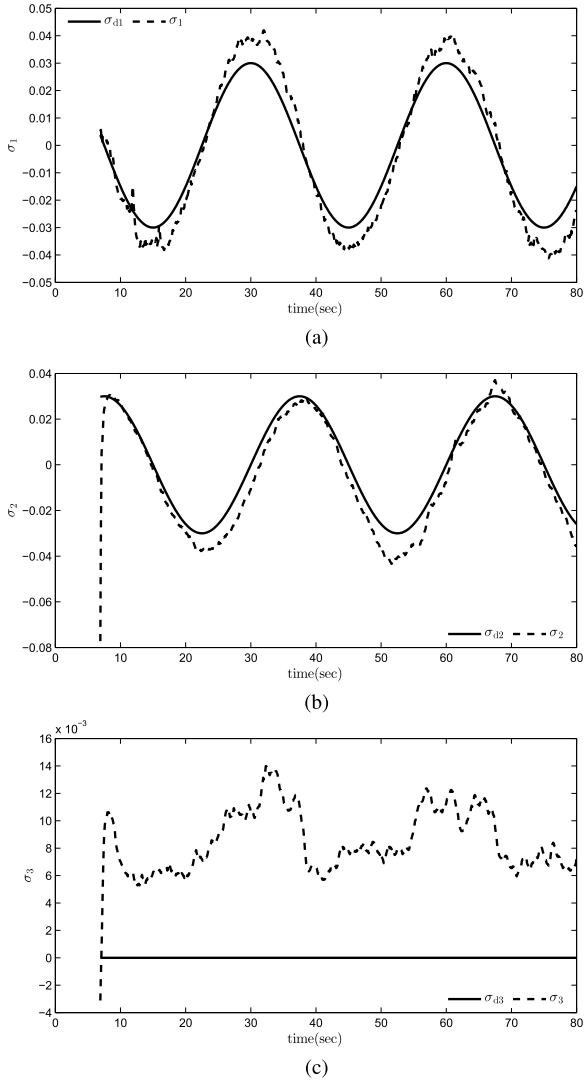

Fig. 5. Tracking effect of MRPs without DOB. (a) Tracking effect of σ_1. (b) Tracking effect of σ_2. (c) Tracking effect of σ_3.

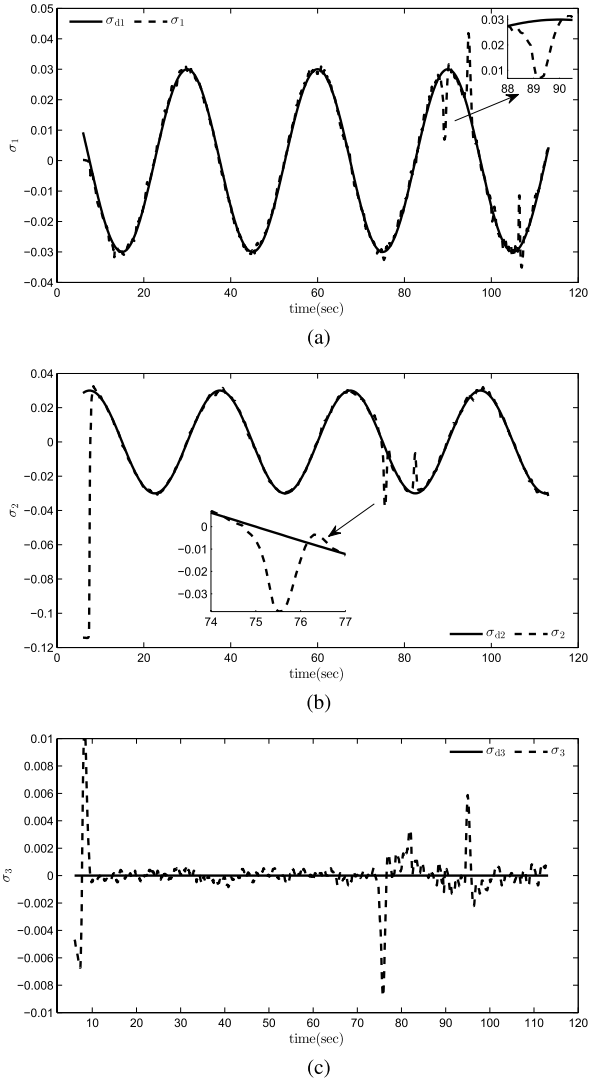

Fig. 6. Tracking effect of MRPs with DOB. (a) Tracking effect of σ_1. (b) Tracking effect of σ_2. (c) Tracking effect of σ_3.

the attitude error can converge with the existence of external disturbances. From the experimental results, the external disturbances will bring the system with MRPs error of about 0.02. However, the designed DOB can estimate the disturbance quickly, with response time less than 2 s.

C. Attitude Tracking

The experiment of attitude tracking is accomplished, while the desired attitude is expressed as follows:

$$\sigma_{d1} = 0.03\cos\left(\frac{\pi}{15}t\right), \quad \sigma_{d2} = 0.03\sin\left(\frac{\pi}{15}t\right) \tag{41}$$

and σ_{d3} retains 0. ω_d and $\dot{\omega}_d$ are acquired from the kinematics of MRPs as

$$\begin{cases} \boldsymbol{\omega}_d = G^{-1}(\boldsymbol{\sigma}_d)\dot{\boldsymbol{\sigma}}_d \\ \dot{\boldsymbol{\omega}}_d = G^{-1}(\boldsymbol{\sigma}_d)[\ddot{\boldsymbol{\sigma}}_d - \bar{G}(\boldsymbol{\sigma}_d, \dot{\boldsymbol{\sigma}}_d)\boldsymbol{\omega}_d] \end{cases} \tag{42}$$

where $\bar{G}(\boldsymbol{\sigma}_d, \dot{\boldsymbol{\sigma}}_d)$ is the time derivative of $G(\boldsymbol{\sigma}_d)$.

From Fig. 5, we find that although there is no external disturbance, the internal uncertainties also lead to the existence of tracking error. This can be easily shown in (9) and (10) that

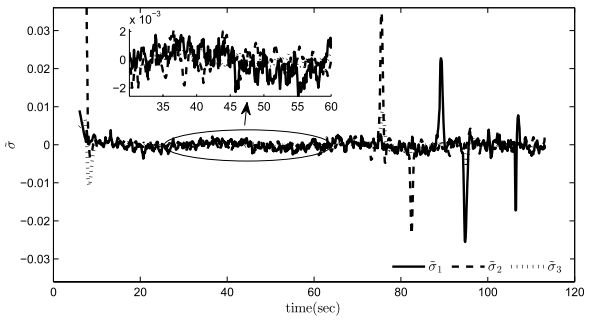

Fig. 7. Tracking error of the proposed scheme.

even if there are no external disturbances, the existing internal uncertainties will also bring the system with an equivalent disturbance $\boldsymbol{f}$. At 75 and 90 s, external disturbances are exerted on the quadrotor. In Fig. 6, we find that with the action of DOB, the tracking error caused by internal uncertainties can be suppressed successfully. From the enlarged view of Fig. 6, the convergence speed of DOB is less than 2 s. The attitude errors are expressed in Fig. 7 and the comparison of the

TABLE II
COMPARISON OF CONTROL PERFORMANCE (RMS ERROR)

	σ_1	σ_2	σ_3
Without DOB	7.1×10^{-3}	7.7×10^{-3}	8.8×10^{-3}
With DOB	7.9×10^{-4}	7.1×10^{-4}	2.9×10^{-4}

attitude tracking performance is shown in Table II. The control accuracy is much higher with the proposed DOB. Meanwhile, from the enlarged view of Fig. 7, the tracking error of both pitch and roll axes are also sine and cosine signals with the same period as desired attitude. This is because DOB cannot suppress the time-varying component of equivalent disturbance completely. Since there exists property of coupling among the 3 DOF of the attitude, when we exert external disturbances on the axes of pitch or roll, it will in turn affect the other 2 DOF. However, the proposed DOB can also suppress the influence caused by coupling property. The experimental results show that the proposed scheme possesses strong disturbance rejection performance against external disturbances as well as good tracking performance.

V. CONCLUSION

This brief proposes a disturbance rejection control strategy for the attitude tracking of an aircraft. We first establish the attitude tracking error model based on MRPs with actuators' uncertainties. A disturbance rejection control scheme is proposed with a well-designed robust DOB and a nonlinear feedback controller. The experimental results validate that the designed control scheme can stabilize the system quickly and accurately. The directly designed DOB can eliminate the external disturbances effectively under the condition of guaranteeing the robust stability. Meanwhile, the quick convergence of DOB makes it practical in systems with requirements of rapidity.

REFERENCES

[1] A. Tayebi and S. McGilvray, "Attitude stabilization of a VTOL quadrotor aircraft," *IEEE Trans. Control Syst. Technol.*, vol. 14, no. 3, pp. 562–571, May 2006.

[2] R. Schlanbusch, E. I. Grøtli, A. Loria, and P. J. Nicklasson, "Hybrid attitude tracking of rigid bodies without angular velocity measurement," *Syst. Control Lett.*, vol. 61, no. 4, pp. 595–601, 2012.

[3] T. Lee, "Exponential stability of an attitude tracking control system on SO(3) for large-angle rotational maneuvers," *Syst. Control Lett.*, vol. 61, no. 1, pp. 231–237, 2012.

[4] H. Du, S. Li, and C. Qian, "Finite-time attitude tracking control of spacecraft with application to attitude synchronization," *IEEE Trans. Autom. Control*, vol. 56, no. 11, pp. 2711–2717, Nov. 2011.

[5] N. M. Horri and P. Palmer, "Practical implementation of attitude-control algorithms for an underactuated satellite," *J. Guid. Control Dyn.*, vol. 35, no. 1, pp. 40–50, 2012.

[6] B. Xiao, Q. Hu, and Y. Zhang, "Adaptive sliding mode fault tolerant attitude tracking control for flexible spacecraft under actuator saturation," *IEEE Trans. Control Syst. Technol.*, vol. 20, no. 6, pp. 1605–1612, Nov. 2012.

[7] L. Wang and H. Jia, "The trajectory tracking problem of quadrotor UAV: Global stability analysis and control design based on the cascade theory," *Asian J. Control*, vol. 16, no. 2, pp. 574–588, 2014.

[8] C. Nicol, C. J. B. Macnab, and A. Ramirez-Serrano, "Robust adaptive control of a quadrotor helicopter," *Mechatronics*, vol. 21, no. 6, pp. 927–938, 2011.

[9] B. Zheng and Y. Zhong, "Robust attitude regulation of a 3-DOF helicopter benchmark: Theory and experiments," *IEEE Trans. Ind. Electron.*, vol. 58, no. 2, pp. 660–670, Feb. 2011.

[10] H. Liu, G. Lu, and Y. Zhong, "Robust LQR attitude control of a 3-DOF laboratory helicopter for aggressive maneuvers," *IEEE Trans. Ind. Electron.*, vol. 60, no. 10, pp. 4627–4636, Oct. 2013.

[11] C. Liu, W.-H. Chen, and J. Andrews, "Tracking control of small-scale helicopters using explicit nonlinear MPC augmented with disturbance observers," *Control Eng. Pract.*, vol. 20 no. 3, pp. 258–268, 2012.

[12] A.-M. Zou, K. D. Kumar, Z.-G. Hou, and X. Liu, "Finite-time attitude tracking control for spacecraft using terminal sliding mode and Chebyshev neural network," *IEEE Trans. Syst., Man, Cybern. B, Cybern.*, vol. 41, no. 4, pp. 950–963, Aug. 2011.

[13] A.-M. Zou and K. D. Kumar, "Adaptive fuzzy fault-tolerant attitude control of spacecraft," *Control Eng. Pract.*, vol. 19, no. 1, pp. 10–21, 2011.

[14] K. Ohnishi, "A new servo method in mechatronics," *Trans. Jpn. Soc. Elect. Eng.*, vol. 107-D, no. 1, pp. 83–86, 1987.

[15] D. Xing, J. Su, Y. Liu, and J. Zhong, "Robust approach for humanoid joint control based on a disturbance observer," *IET Control Theory Appl.*, vol. 5, no. 14, pp. 1630–1636, Sep. 2011.

[16] J. Yang, S. Li, X. Chen, and Q. Li, "Disturbance rejection of dead-time processes using disturbance observer and model predictive control," *Chem. Eng. Res. Design*, vol. 89, no. 2, pp. 125–135, 2011.

[17] W. Li and Y. Hori, "Vibration suppression using single neuron-based PI fuzzy controller and fractional-order disturbance observer," *IEEE Trans. Ind. Electron.*, vol. 54, no. 1, pp. 117–126, Feb. 2007.

[18] S.-H. Lee, H. J. Kang, and C. C. Chung, "Robust fast seek control of a servo track writer using a state space disturbance observer," *IEEE Trans. Control Syst. Technol.*, vol. 20, no. 2, pp. 346–355, Mar. 2012.

[19] Z.-J. Yang, Y. Fukushima, and P. Qin, "Decentralized adaptive robust control of robot manipulators using disturbance observers," *IEEE Trans. Control Syst. Technol.*, vol. 20, no. 5, pp. 1357–1365, Sep. 2012.

[20] J. N. Yun, J. Su, Y. I. Kim, and Y. C. Kim, "Robust disturbance observer for two-inertia system," *IEEE Trans. Ind. Electron.*, vol. 60, no. 7, pp. 2700–2710, Jul. 2013.

[21] J. Su, L. Wang, and J. N. Yun, "A design of disturbance observer in standard H_∞ control framework," *Int. J. Robust Nonlinear Control*, doi: 10.1002/rnc.3235.

[22] J. C. Doyle, K. Glover, P. P. Khargonekar, and B. A. Francis, "State-space solutions to standard H_2 and H_∞ control problems," *IEEE Trans. Autom. Control*, vol. 34, no. 8, pp. 831–847, Aug. 1989.

[23] P. Tsiotras, "Further passivity results for the attitude control problem," *IEEE Trans. Autom. Control*, vol. 43, no. 11, pp. 1597–1600, Nov. 1998.

[24] B.-L. Cong, X.-D. Liu, and Z. Chen, "Distributed attitude synchronization of formation flying via consensus-based virtual structure," *Acta Astron.*, vol. 68, nos. 11–12, pp. 1973–1986, 2011.

[25] H. K. Kahlil, *Nonlinear Systems*, 3rd ed. Upper Saddle River, NJ, USA: Prentice-Hall, 2002.

[26] R. Mahony, T. Hamel, and J.-M. Pflimlin, "Nonlinear complementary filters on the special orthogonal group," *IEEE Trans. Autom. Control*, vol. 53, no. 5, pp. 1203–1218, Jun. 2008.